Analysis of an Electrocardiographic Multilead System by Means of Artificial Neural Networks
Study of Repolarization During Premature Ventricular Stimulation

Drago Torkar[1] and Pedro David Arini[2,3]

[1]*Jožef Stefan Institute, Jamova Cesta 39, 1000 Ljubljana, Slovenia*
[2]*Instituto de Ingeniería Biomédica, Facultad de Ingeniería, Universidad de Buenos Aires, Buenos Aires, Argentina*
[3]*Instituto Argentino de Matemática, 'Alberto P. Calderón' CONICET, Buenos Aires, Argentina*

Keywords: Electrocardiography, Transmural Dispersion, Mapping, ANN, Pacing.

Abstract: The ventricular repolarization dispersion (VRD) has been shown to increase with premature stimulation. Moreover, several differences between left ventricular and right ventricular, such as the anatomic properties and fibrillation threshold have been reported. However, few data exist regarding the influence of the site of stimulation on modulation of VRD measure by electrocardiographic. In the present work, several ECG indices of VRD, as a function of the coupling interval and the site of stimulation, were studied in an isolated heart rabbit preparation (n=18), using ECG multilead (5 rows x 8 columns) system with Artificial Neural Networks. In both ventricles, results have shown significant decreases in early repolarization duration, while in the left ventricle we have found significant increases of transmural dispersion. Also, we have observed that when the premature stimuli were applied to the left ventricle, the ventricular repolarization dispersion changes were detected using only one preferential electrode (row1-column3). When stimuli were elicited at the right ventricle, changes of VRD were detected by three electrodes (row3-column1, row2-column1 and row3-column8). Finally, a different ventricular repolarization dispersion was found as a function of the site of stimulation.

1 INTRODUCTION

Heterogeneity of ventricular repolarization is a measure of nonhomogeneous recovery of excitability during the repolarization phase. This ventricular heterogeneity is mainly attributable to differences in activation times and action potential duration (APD) in different myocardium areas. The APDs differs not only between cardiac cells of different ventricular layers (Yan and Jack, 2003) but also between posterior and anterior endocardial layers, apex and base (Noble and Cohen, 1978), and left and right ventricles (Di Diego et al., 1996).

Clinical and experimental studies have shown a relationship between ventricular repolarization dispersion (VRD) and severe ventricular arrhythmia and/or sudden cardiac death (Surawicz, 1997) (Kuo et al., 1983). In this way, changes in VRD values that are higher than normal have been linked with an increased risk of developing reentrant arrhythmias (Han and Moe, 1964; Shimizu and Antzelevitch, 1998).

Some authors have shown that alterations in VRD are correlated with changes in the total repolarization duration (T_{RD}) or T-wave width (Fuller et al., 2000). Our study has also shown that T-wave widening can result from a differential shortening or lengthening of the APD in both apex-base and transmural (Arini et al., 2008). Moreover, the T-wave peak-to-end (T_{PE}) interval has been suggested as a marker of transmural repolarization dispersion (Antzelevitch et al., 2007; Smetana et al., 2011), consequently the interval between the J-point and the T-wave peak position has been considered as the full repolarization of epicardium or early repolarization duration (E_{RD}). The translation of these concepts to the standard ECG is not straightforward, making it difficult the interpretation of the relationship between T-wave peak-to-end and transmural dispersion in a clinical population (Smetana et al., 2011).

In this regard, several investigations showed that premature ventricular stimulation (PVS) produce a significantly increased of the VRD and that these changes were markedly associated with an increase in the induction of ventricular arrhythmias (Kuo et al., 1985; Rosenbaum et al., 1991; Yuan et al., 1996). Also, ventricular vulnerability, as evaluated

by the ventricular fibrillation threshold technique, was shown different when studied at the left ventricle (Lv) or at the right ventricle (Rv). The left ventricular epicardium presented higher fibrillation threshold when compared with left ventricular endocardium or both epicardium and endocardium of right ventricular, respectively (Horowitz et al., 1981).

Because a different ventricular fibrillation threshold and differences in the anatomic properties may exist between both ventricles, we hypothesized that there also would be differences in the E_{RD}, T_{PE} and T_{RD} values depending on the site where premature ventricular stimuli were elicited.

The aims of this work were to: (1) Determine the preferential electrode, in a multilead ECG system, to detect changes of ventricular repolarization dispersion using Artificial Neural Networks. (2) Evaluate ECG indices associated to the ventricular repolarization dispersion depending on the site of pacing during premature ventricular stimulation.

2 MATERIALS AND METHODS

2.1 Isolated Heart Rabbit Preparation

This study conformed to the *Guide for the Care and Use of Laboratory Animals* published by the US National Institutes of Health (NIH Publication No. 85-23, revised 1996). To obtain isolated Langendorff-perfused rabbit hearts, male New Zealand white rabbits of 2.8-3.8 Kg (n = 18) were heparinized (500 U/Kg IV) and anesthetized by the intramuscular injection of a combination of lidocaine (5 mg/Kg) and ketamine (35 mg/Kg). The rabbits were euthanized by cervical dislocation. The chest was opened via a median sternotomy and, immediately, the heart was removed with scissors and immersed in cold Tyrode's solution. After the remaining connective tissue, lungs, and pericardium were removed, the heart was placed in a vertical Langendorff device through cannulation of the aorta. Time from chest opening to cannulation of the aorta oscillated between 2 to 3 minutes. The heart was retrogradely perfused through the aorta with Tyrode's solution and immersed in a tank filled with the same solution (Zabel et al., 1995). The temperature of both solutions were maintained at $38^o \pm 0.5^o$C and bubbled with O_2 using a flow of 700-900 ml/h at a pressure of 70 mmHg. To regulate the flow rate of the aortic perfusion, a variable speed roller pump (Extracorporeal, 2102 Infusion Pump) was used. Care was taken to fix the hearts in the same position by alignment of the left anterior descending coronary artery (LAD) with the electrode matrix reference system on the tank (see Figure 1).

The composition of Tyrode's solution was (in mM): 140 NaCl, 5 KCl, 1 $MgCl_2$, 0.33 NaH_2PO_4, 5 Hepes, 11.1 glucose and 2 $CaCl_2$. The pH was adjusted to 7.4 using NaOH. The sinus node was destroyed by applying radiofrequency energy through a customized device.

The artificial pacemaker was a rectangular pulse that had a 2 ms duration and twice the diastolic threshold stimuli amplitude. In the premature ventricular stimulation (PVS) experimental protocol, the bipolar pacing electrodes made of Teflon-coated stainless-steel wires were positioned in the middle of the base of each ventricle, below the auricle appendage (Figure 1). To ensure stability in the preparation, the heart activity was monitored for 30 min to determine that the heart was arrhythmia-free, stable in amplitude, and had no manifest ischemia. We used an In Vitro rabbit heart model because it provides advantages such as a high level of experimental reproducibility, has a greater throughput compared to complicated in vivo models, provides a better evaluation over a range of concentrations and different combinations of drugs to be tested. In addition, it can be manipulated to mimic clinical conditions, such as hypokalemia and bradycardia that support these comments. Also, it has been well established that with PVS beats (Laurita et al., 1998) a significant increase in ventricular repolarization dispersion is induced.

2.2 Thorax Rabbit Model

The experimental model consisted of the In Vitro system, which used a multiple recording system to obtain the beat-to-beat electrical activity of isolated rabbit heart. The PVS protocol used a circular tank (diameter = 7 cm, height = 7 cm) that had 40 silver-silver chloride electrodes (diameter = 2 mm) distributed homogeneously within an array of 5 rows and 8 columns (see Figure 1). The distance between electrodes was 10 mm and the angular distance was 45°. The dimensions of the tank simulated a rabbit's thorax. Four additional electrodes were allocated in an *"Einthoven-like"* configuration (Figure 1). Two of them were positioned on the base of the tank and the other two were on the upper left and right side of the tank wall and served as arm electrodes. The four electrodes were designed to build the electrical reference by configuring the Wilson Central Terminal.

2.3 Experimental Protocol

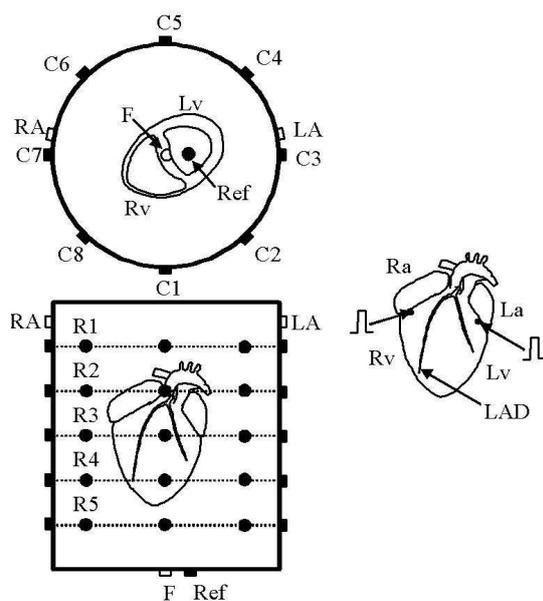In this study VRD was modified by premature ventricular stimulation. Due to heterogeneous distribution

Figure 1: ECG multilead system: 40-electrodes configuration for electrocardiographic recording in the premature ventricular stimulation protocol. Schematic view showing the superior and frontal 5×8 matrix electrodes, as well as the standard lead foot (F), left arm (LA), right arm (RA), and reference (Ref). Also are shown the positions of both the stimulating electrodes located in the base of the Lv and Rv, below the atrial appendages.

of APD lengthening induced by potassium-channel blocking drugs (Zabel et al., 1997; Spear and Moore, 2000) or the heterogeneous shortening of APD caused by the heterogeneous distribution of restitution kinetics (Laurita et al., 1998), a real increase in VRD phenomena can be obtained. Besides, it can be noted that we measured the increase in VRD, not dispersion as an absolute value, so our gold standard was the same heart in the control condition in each experiment.

In the PVS protocol, the heart was stimulated from the right ventricle (Rv) or left ventricle (Lv) at basal frequency during a train (S1) of 49 beats. After that train, at beat number 50th, a premature beat was generated at a coupling interval that corresponded to the Effective Refractory Period (E_{rp}) plus 5 ms. In each case, E_{rp} was estimated prior to the PVS application. To estimate E_{rp}, premature coupling intervals (distance from the last beat to the premature stimulation time) were diminished step by step at 5 ms until period refractoriness was reached. We used the average of 48th and 49th beats from each S1 as control. The premature beat (50th) was elicited to generate VRD paced either at Rv or Lv. During the protocol, the heart was paced using an artificial pacemaker (DTU 101, Bloom Associates Ltd. Reading, PA, USA).

In the PVS protocol (n = 18), the hearts were paced from the Rv (n = 9) or the Lv (n = 9) by stimuli trains at a basic cycle length of 430 ms for control condition. Then, single premature stimuli were applied after a pulse train at a frequency equal to E_{rp}+5 ms (167±7.2 ms for Rv stimulation (RVS) and 168±11.5 ms for Lv stimulation (LVS); p value = NS).
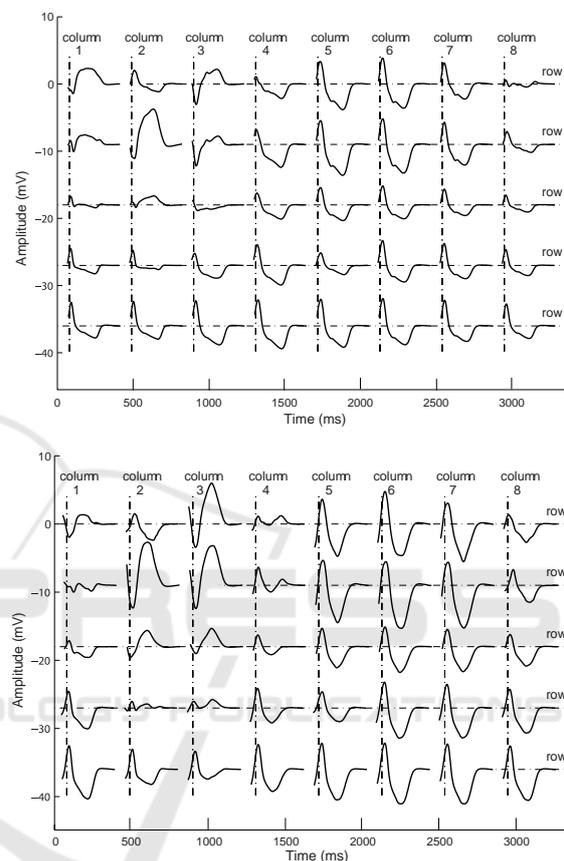

Figure 2: 40 ECG recordings from the control situation (top panel) and their respective E_{rp}+5 ms (bottom panel) during PVS from the left ventricle. The stimulating electrode was located at the base of the left ventricle.

2.4 Acquisition of ECGs Signals

ECG data were recorded using instrumentation amplifiers that had a gain factor of 1000 and a bandwidth of 0.05-300 Hz. The signals were digitalized at a sampling rate $f_s = 1$ KHz and 12-bit resolution using a digital acquisition board (Lab PC+, National Instruments, Austin, TX, USA). When necessary, a band-stop filter was used to remove 50-Hz. The baseline movement was compensated using a cubic spline (Meyer and Keiser, 1977) algorithm. All of the data were acquired and monitored using customized software made in C++.

2.5 Construction of Data Matrix

The ECGs from the first row of leads were recorded simultaneously, and the same procedure was applied sequentially to the remaining rows. The ith beat was selected in the ECG recordings of each rth row, $r = 1,\ldots,5$, obtaining the i_r^{th} beat. After selecting and segmenting the i_r^{th} beat from each row, a signal, $x_{c,r}(n)$, $n = 0,\ldots,N-1$, was determined for each channel characterized by the (c,r) pair, where c is the column in the electrode matrix ($c = 1,\ldots,8$) and r is the row. , being $M = 5 \times 8$ the number of register electrodes in each experimental protocol, respectively. Expressing that signal as a vector, $\mathbf{x}_{c,r}$, we obtain

$$\mathbf{x}_{c,r} = [x_{c,r}(0),\ldots,x_{c,r}(N-1)]^T \quad (1)$$

The five i_r^{th} selected beats were aligned using the QRS complex maximum upstroke slope. The beats extend a time window composed of N samples corresponding to 400 ms, and include the repolarization phase. For each experimental condition (control and $E_{rp}+5$ ms), recordings were obtained from 40 ECG leads for the experimental protocol. Expressing in matrix notation the selected segmented signals, $\mathbf{X}$ ($M \times N$), we obtain

$$\mathbf{X} = [\mathbf{x}_{1,1},\ldots,\mathbf{x}_{L,1},\ldots,\mathbf{x}_{1,5},\ldots,\mathbf{x}_{L,5}]^T \quad (2)$$

From $\mathbf{X}$, the ECG-derived parameters were measured. A matrix $\mathbf{X}$ characterize each experimental condition.

2.6 ECG Indices

The QRS fiducial points (QRS_{ON} and QRS_{END}) and T-wave location (T_{END}, T_{PEAK}) were obtained from the ECG delineation system based on the Wavelet Transform (Mendieta, 2012). Also, ECG indices have been computed to describe the characteristics of VRD on the electrocardiographic multilead system. For each ith beat, we have computed as:

1) Ventricular depolarization index: the Q_{RS} interval measured in milliseconds from the onset of the Q wave to the offset of the S wave, has been calculated as;

$$Q_{RS_i} = QRS_{END_i} - QRS_{ON_i} \quad (3)$$

2) Total ventricular repolarization duration index (measured in milliseconds): the T_{RD} quantifying the total ventricular repolarization time, has been computed as;

$$T_{RD_i} = T_{END_i} - QRS_{END_i} \quad (4)$$

3) Early repolarization duration index (measured in milliseconds): the E_{RD} which several authors have linked to the full repolarization of epicardium, has been calculated as;

$$E_{RD_i} = T_{PEAK_i} - QRS_{END_i} \quad (5)$$

4) T-wave peak-to-end interval index (measured in milliseconds): the T_{PE} associated to transmural ventricular repolarization (Antzelevitch et al., 2007), has been computed as;

$$T_{PE_i} = T_{END_i} - T_{PEAK_i} \quad (6)$$

2.7 Artificial Neural Network

The measured ECG indices depend on the premature coupling interval between S1 pulse train and the premature beat. The question is, if it is possible to recognize the coupling interval from ECG values, or in other words how successfully we can separate ECG indices values corresponding to $E_{rp}+5$ ms coupling interval from those corresponding to control stimulation. Furthermore, we wanted to know the signals from which electrodes can be most successfully classified, since this would indicate the preferential electrode positions in the tank (thorax rabbit model) most suitable to perform measurements. There were 572 samples from 9 rabbit hearts (63.5 samples/heart) for Lv stimulation (LVS) and 535 samples also from 9 rabbit hearts (59.4 samples/heart) for Rv stimulation (RVS) available. The data was reasonably balanced with 50.87% $E_{rp}+5$ ms and 49.13% control samples in Lv stimulation data, and 48.22% $E_{rp}+5$ ms and 51.78% control samples in Rv stimulation data. The LVS and RVS data were processed separately. Each dataset was divided into 3 sets: the training set (60%), the cross-validation set (20%) and the test set (20%).

Table 1: Lv stimulation (LVS) and Rv stimulation (RVS) ANN parameters determined by genetic algorithm after 100 generations. Step size 1 refers to weights between input and hidden layer, step size 2 refers to weights between hidden and output layer.

	LVS	RVS
hidden layer neurons	25	21
step size 1	0.07	0.49
step size 2	0.41	0.44
momentum rate	0.70	0.70

The two class classification procedure was performed by employment of artificial neural networks (ANN). We used a multi-layered perceptron with one hidden layer and a backpropagation training algorithm. This is a fully connected feed-forward only ANN architecture with weighted neuron connections from the input towards the output (Figure 3).
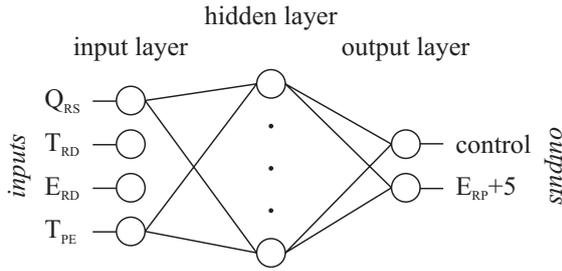
Figure 3: ANN topology with input and output signals used for classification of ECG data.

During the training process these weights are automatically adjusted by a backpropagation algorithm so that the difference between the actual and the desired output is minimal. The momentum learning rule and the logistic sigmoid transfer function were applied in all layers.The number of hidden layer neurons, the learning step size and the momentum rate were determined using optimization with genetic algorithm (see Table 1).

The input data was randomized before training. The genetic optimization took place throughout 100 generations. In every genetic iteration the ANN was trained with 1000 epochs. The ANN outputs correspond to an individual class and each one produces a numbers between 0 and 1. The posterior decision function classified a particular sample into the class which corresponded to the output that had bigger value. The classification score was measured by the standard measure: classification accuracy (Eq. 7), calculated from 4 standard quantities: true positive (TP), true negative (TN), false positive (FP), false negative (FN). Other standard measures like sensitivity, specificity and precision take the same values due to a two class problem and the selected decision function. The whole training and the classification of all available data was repeated ten times and the results were averaged.

$$CA = \frac{(TP + TN)}{(TP + TN + FP + FN)} \qquad (7)$$

Classification accuracy was then calculated for each measuring electrode and the ones with the best scores were identified as preferential. The contour maps were generated using these classification scores showing the preferential areas in the matrix of electrodes.

2.8 ECG Recording Stability

To quantify the stability of ECG recordings we have measured the coefficient of variation (C_V) parameter (Rosner, 1994) for each feature, the Q_{RS}, T_{RD}, E_{RD}

and T_{PE}. These variables were repeatedly measured at each electrode of the multi-lead ECG recording system every 20 min during an hour.

The C_V is defined as

$$C_V = \sqrt{\sigma^2} \times 100\% \qquad (8)$$

and the σ^2 (variance within) is estimated as

$$\sigma^2 = \sum_{i=1}^{k} \sum_{j=1}^{n_i} \frac{(y_{ij} - \bar{y}_i)^2}{n - k} \qquad (9)$$

For each variable evaluated (Q_{RS}, T_{RD}, E_{RD} and T_{PE}) we assume that there are k groups of measurements with n_i measurements in the ith group. The jth measurements in the ith group will be denoted by y_{ij} and $n = \sum_{i=1}^{k} n_i$. The term $(y_{ij} - \bar{y}_i)$ represents the deviation of an individual measurement from the group mean for that measurement and is a clue of within group variability.

2.9 Statistical Analysis

In order to quantify the discrepancy between the parameters' distribution and the Gaussian distribution, we have analyzed the normality of these values using the D'AgostinoPearson test. It has been observed that the underlying variables'distribution was Gaussian. Data were expressed as mean value ± standard deviation (SD). Comparison between ECG indices were performed by means of paired or unpaired Student t-test for normally distribution variables. Significance was considered at a value of $p < 0.05$.

3 RESULTS

In some experiments, we have evaluated the C_V for each variable. The C_V was $< 2\%$ for Q_{RS}, $< 2\%$ for E_{RD}, $< 3\%$ for T_{PE} and $< 3\%$ for T_{RD}. So, we have verified that the estimated variables have not shown significant statistical differences over the 1-h In Vitro experiment.

It can be observed in Figure 2, a representative example the 40 ECG recordings from the control situation and its respective premature ventricular stimulation at $E_{rp}+5$ ms from the left ventricle.

The classification results have shown that there is one preferential electrode during LVS. It has been located in row #1 and column #3 and so called as r1c3. Moreover, we have observed three preferential electrodes during RVS. These have been located in row #3 and column #1 (denominated as r3c1); row #2 and column #1 (so called as r2c1) and row #3 and column #8 (denominated as r3c8).

Table 2: Mean values $\pm$ standard deviation of the experiments (n=8 during LVS and n=9 during RVS) showing all dispersion ECG indices measured in control and in E_{rp}+5 ms. The values were computed in the preferential electrodes during stimulation in Lv (n=8) and Rv (n=9), respectively.

	control	E_{rp}+5 ms.	stimulation site	preferential electrode	p-value
Q_{RS}	76.50±7.33	100.13±85.50	Lv	r1c3	0.0006
	76.50±6.37	105.00±17.02	Rv	r3c1	0.0002
	73.00±10.17	101.33±18.61	Rv	r2c1	0.0470
	72.11±6.07	99.50±20.35	Rv	r3c8	0.0015
E_{RD}	119.00±17.70	85.50±21.42	Lv	r1c3	0.0018
	114.14±17.09	107.50±8.54	Rv	r3c1	NS
	115.50±15.02	85.67±0.58	Rv	r2c1	0.0202
	122.63±18.30	94.40±26.82	Rv	r3c8	0.0441
T_{PE}	52.38±5.07	72.13±21.26	Lv	r1c3	0.0201
	57.57±18.37	57.25±15.39	Rv	r3c1	NS
	58.00±7.62	79.67±15.04	Rv	r2c1	NS
	54.75±9.62	56.00±17.16	Rv	r3c8	NS
T_{RD}	171.38±18.15	157.63±16.75	Lv	r1c3	0.0019
	173.50±15.57	158.50±18.09	Rv	r3c1	NS
	173.50±10.79	165.33±15.01	Rv	r2c1	NS
	174.67±20.21	153.75±18.07	Rv	r3c8	0.0409

Mean and standard deviation of Q_{RS}, T_{RD}, E_{RD} and T_{PE} indices during the control condition and during LVS and RVS are presented in Table 2. It can be observed that these results were computed for preferential leads in each kind of stimulation, LVS and RVS respectively.

On the other hand, with the aim to localize the spatial position of the preferential electrode in the 5 x 8 matrix electrodes, we have shown a colored contour maps, as we can see in Figure 4.

We have tested the trained ANNs with all the datasets available (Table 3). The lowest classification accuracy achieved was on the test set of LVS data which is expected since the test set was not exposed to ANN during training. The RVS data exhibit better result on all datasets used. One reason for this might be better quality of RVS measurements in comparison to LVS measurements. All available data has been used to calculate the CA of every individual electrode. The preferential electrodes exhibited 100% CA which means that the signals from these electrodes can be certainly distinguished one from another at all times and thus they show the ventricular repolarization activity most clearly. This is our most important result obtained.

4 DISCUSSION

A total of 40 unipolar leads, in 18 isolated heart rabbit preparation, were studied using Artificial Neural Networks with the aim to analyze: the preferential electrode to detect VRD during premature stimuli (E_{rp}+5

Table 3: Classification accuracy (CA) for different data sets, Lv stimulation (LVS) and Rv stimulation (RVS).

dataset	CA LVS	CA RVS
training set	0.83	0.86
cross-validation	0.85	0.89
test	0.78	0.87
all data	0.82	0.87

ms) and evaluate which ECG indices are dependent on the site of pacing during premature ventricular stimulation.

We have observed that when the premature stimuli were applied to the Lv, the VRD changes were detected using only one preferential electrode (r1c3). When stimuli were elicited at the Rv, changes of VRD were detected by three electrodes (r3c1, r2c1 and r3c8). Moreover, we have observed that preferential electrode during stimulation of Lv is located opposite of this ventricle. At the same way the preferential electrodes during stimulation of Rv are located exactly opposite of the right ventricle. It can be observed these positions in Figure 1. Also, it is important to highlight that all hearts were fixed in the same position, as we have describe in Section 2.1.

Otherwise, we have observed, in both Lv or Rv premature stimulation (E_{rp}+5 ms), a statistical significant increase of Q_{RS} index duration (see Table 2). We have concluded that depolarization cardiac phase did not seem to be different when the stimuli were elicited from either the Lv or Rv, because both ventricles exhibited a similar response to the premature ventricular stimulation.
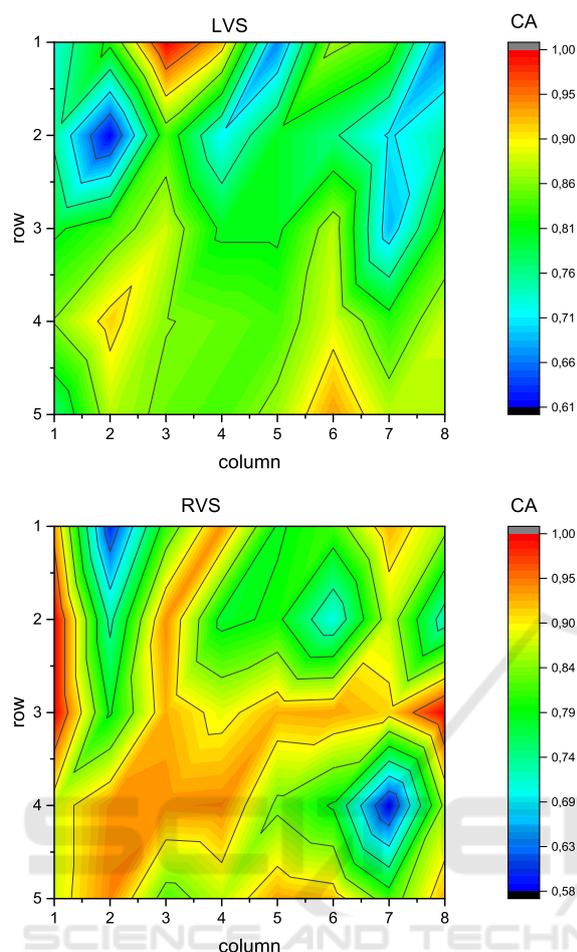
Regarding the T_{PE} index, associated to transmu-

Figure 4: Contour maps of accuracies (CA) distributed over the 5x8 matrix electrodes. Top panel: one preferential electrode during Lv stimulation (LVS), located in row #1 and column #3 (red area). Bottom panel: three preferential electrodes during Rv stimulation (RVS), located in row #3 and column #1, row #2 and column #1 and row #3 and column #8 (red area).

ral ventricular repolarization dispersion, we have only found statistically significant increases during premature stimuli (E_{rp}+5 ms.) in the Lv (see Table 2). Moreover, the E_{RD} index have shown statistically significant decreases in premature ventricular stimulation of the Lv and the Rv (except in electrode r3c1, see Table 2). Conversely, no significant changes in T_{RD} (only in r3c8 and with a p-value near to 0.05) has been observed. We denoted that the T_{RD} index did not change because the T_{PE} index increase and E_{RD} decrease its values, simultaneously (see Table 2).

Artificial neural network is one of the machine learning classification tools which are most widely used in biomedical applications due to good results obtained (Dreiseitl and Ohno-Machado, 2002; Cai and Jiang, 2014; Chen et al., 2015; Shaikhina et al., 2015). It is a nonlinear non-parametric model which can mimic from very simple to very complex problems. It possesses ability to implicitly detect complex nonlinear relationships between dependent and independent variables. The electrocardiographic multilead system seems to be an appropriate one to be analysed by ANN. Of course, we could have picked some other classification algorithm but since there is no way to select the most suitable method in advance there should be performed a thorough comparison of the methods which is beyond the scope of this paper and is left for future work.

Moreover, the mechanism responsible for different response by premature stimulation depending on the site of pacing is not clearly explainable only with the present results. There are anatomic differences between ventricles, such as the 3D structure or the anisotropic properties linked with dissimilar wall thickness and cardiac fibers orientation. We have concluded that all of these parameters might contribute to the different results obtained between both ventricles. Finally, the present results have shown that changes of VRD during premature stimuli can be very well captured by means of artificial neural networks in a multilead ECG system

5 STUDY LIMITATIONS

No attempt was made to measure ventricular repolarization dispersion on the epicardial surface or endocardial muscle layers. We have limited our analysis to ECG signals obtained from recording electrodes embedded in the tank wall.

6 CONCLUSIONS

During premature ventricular stimulation we have observed significant decreases in early repolarization duration for both ventricles, while in the Lv we have observed significant increases of transmural dispersion. Moreover, we have found preferential electrodes to detect VRD, when the premature ventricular stimuli were elicited from left or right ventricles.

ACKNOWLEDGEMENTS

REFERENCES

Antzelevitch, C., Viskin, S., Shimizu, W., Yan, G., Kowey, P., Zhang, L., Sicouri, S., Di Diego, J., and Burashnikov, A. (2007). Does Tpeak-Tend provide an index of transmural dispersion of repolarization? *Hearth Rhythm*, 4(8):1114–1119.

Arini, P. D., Bertrán, G. C., Valverde, E. R., and Laguna, P. (2008). T-wave width as an index for quantification of ventricular repolarization dispersion: Evaluation in an isolated rabbit heart model. *Biomed. Signal Proc. Control*, 3:67–77.

Cai, B. and Jiang, X. (2014). A novel artificial neural network method for biomedical prediction based on matrix pseudo-inversion. *J. of Biomed. Informatics*, 48:114–121.

Chen, F., Pan, Y., Li, K., Cheng, K., and Huan, R. (2015). Standard 12-lead ECG synthesis using a GA optimized BP neural network. *7th International Conference on Advanced Computational Intelligence*, 7:289–293.

Di Diego, J. M., Sun, Z. Q., and Antzelevitch, C. (1996). Ito and action potential notch are smaller in left vs. right canine ventricular epicardium. *A. J. Physiol.*, 271:H548.

Dreiseitl, S. and Ohno-Machado, L. (2002). Logistic regression and artificial neural network classification models: a methodology review. *J. of Biomed. Informatics*, 35:352–359.

Fuller, M. S., Sándor, G., Punske, B., Taccardi, B., MacLeod, R. S., Ershler, P. R., Green, L. S., and Lux, R. L. (2000). Estimates of repolarization and its dispersion from electrocardiographic measurements: direct epicardial assesment in the canine heart. *J. of Electrocardiol.*, 33:171–180.

Han, J. and Moe, G. K. (1964). Nonuniform recovery of excitability in ventricular muscle. *Circ. Res.*, 14:44–54.

Horowitz, L., Spear, J., and Moore, E. (1981). Relation of endocardial and epicardial ventricular fibrillation thresholds of the right and left ventricles. *Am. J. Cardiol.*, 48:698–701.

Kuo, C. S., Atarashi, H., Reddy, P., and Suracwicz, B. (1985). Dispersion of ventricular repolarization and arrhythmia: Study of two consecutive ventricular premature complexes. *Circ.*, 72:370–376.

Kuo, C. S., Munakata, K., Reddy, P., and Surawicz, B. (1983). Characteristics and possible mechanism of ventricular arrhytmia dependent on the dispersion of action potential. *Circ.*, 67:1356–1367.

Laurita, K. R., Girouard, S. D., Fadi, G. A., and Rosenbaum, D. S. (1998). Modulated dispersion explains changes in arrhythmia vulnerability during premature stimulation of the heart. *Circ.*, 98:2774–2780.

Mendieta, J. G. (2012). Algoritmo para el delineado de señales ECG en un modelo animal empleando técnicas avanzadas de procesamiento de señales. Master Thesis. , Facultad de Ingeniería de la Universidad de Buenos Aires.

Meyer, C. R. and Keiser, H. t. (1977). Electrocardiogram baseline noise estimation and removal using cubic spline and state-space computation techniques. *Comp. and Biomed. Res.*, 10:459–470.

Rosenbaum, D. S., Kaplan, D. T., Kanai, A., Jackson, L., Garan, H., Cohen, R. J., and Salama, G. (1991). Repolarization inhomogeneities in ventricular myocardium change dynamically with abrupt cycle length shortening. *Circ.*, 84:1333–1345.

Rosner, B. (1994). *Fundamentals of Biostatistics*. Duxbury Press, fourth edition edition.

Shaikhina, T., Lowe, D., Daga, S., Briggs, D., Higgins, R., and Khovanova, N. (2015). Machine learning for predictive modelling based on small data in Biomedical Engineering. *IFAC-PapersOnLine*, 48:469–474.

Shimizu, W. and Antzelevitch, C. (1998). Cellular basis for the ECG features of the LQT1 form of the long QT syndrome. efects of β adrenergic agonist and antagonist and sodium channel blockers on transmural dispersion of repolarization and torsades de pointes. *Circ.*, 98:2314–2322.

Smetana, P., Schmidt, A., Zabel, M., Hnatkova, K., Franz, M., Huber, K., and Malik, M. (2011). Assessment of repolarization heterogeneity for prediction of mortality in cardiovascular disease: peak to the end of the T wave interval and nondipolar repolarization components. *J Electrocardiol*, 44:301–308.

Spear, J. and Moore, E. (2000). Modulation of arrhytmias by isoproterenol in a rabbit heart model of d-Sotalol induced long QT intervals. *American J. Physiol*, (279):H15–H25.

Surawicz, B. (1997). Ventricular fibrillation and dispersion of repolarization. *J. Cardiovasc. Electrophysiol.*, 8:1009–1012.

Noble, D. and Cohen, I. (1978). The interpretation of the T wave of the electrocardiogram. *Cardiovasc. Res.*, 12:13–27.

Yan, G. and Jack, M. (2003). Electrocardiographic T wave: A symbol of transmural dispersion of repolarization in the ventricles. *J. of Cardiovasc. Electrophysiol.*, 14:639–640.

Yuan, S., Blomström-Lundqvist, C., Pherson, C., Wohlfart, B., and Olsson, S. B. (1996). Dispersion of ventricular repolarization following double and triple programmed stimulation: A clinical study using the monophasic action potential recording technique. *Eur. Heart J.*, 17:1080–1091.

Zabel, M., Hohonloser, S. H., Beherens, S., Woosley, R. L., and Franz, M. R. (1997). Differential effects of d-Sotalol, quinidine and amiodarone on dispersion of ventricular repolarization in the isolated rabbit heart. *J. Cardiovascular Electrophysiol.*, 8:1239–1245.

Zabel, M., Portnoy, S., and Franz, M. R. (1995). Electrocardiographic indexes of dispersion of ventricular repolarization: An isolated heart validation study. *J. Am. Coll. Cardiol.*, 25:746–752.